Energy & Environmental Science

Accepted Manuscript

ROYAL SOCIETY OF CHEMISTRY

www.rsc.org/ees

Table of Contents Entry

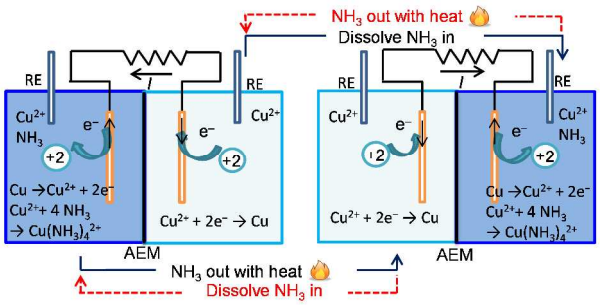

A thermally regenerative ammonia-based battery that was driven by metal ammine complex formation and ammonia concentration gradients to create voltage, showed efficient conversion of low-grade thermal energy into electrical power.

Date: 10/23/2014
Submitted to: *Energy & Environmental Science*

A thermally regenerative ammonia-based battery for efficient harvesting of low-grade thermal energy as electrical power

Fang Zhang, Jia Liu, Wulin Yang and Bruce E. Logan*

Department of Civil and Environmental Engineering, Penn State University,

212 Sackett Building, University Park, PA 16802, USA

* Corresponding Author, blogan@psu.edu;

+1-814-863-7908 (phone), +1-814-863-7304 (Fax)

Abstract

Thermal energy was shown to be efficiently converted into electrical power in a thermally regenerative ammonia-based battery (TRAB) using copper-based redox couples [$Cu(NH_3)_4^{2+}$/Cu and Cu(II)/Cu]. Ammonia addition to the anolyte (2 M ammonia in a copper-nitrate electrolyte) of a single TRAB cell produced a maximum power density of 115 ± 1 W m^{-2} (based on projected area of a single copper mesh electrode), with an energy density of 453 Wh m^{-3} (normalized to the total electrolyte volume, under maximum power production condition). Adding a second cell doubled both the voltage and maximum power production. Increasing the anolyte ammonia concentration to 3 M further improved power density to 136 ± 3 W m^{-2}. Volatilization of ammonia from the spent anolyte by heating (simulating distillation), and re-addition of this ammonia to the spent catholyte chamber with subsequent operation of this chamber as the anode (to regenerate copper on the other electrode), produced a power density of 60 ± 3 W m^{-2}, with an average

discharge energy efficiency of ~29% (electrical energy captured versus chemical energy in the starting solutions). Power was restored to 126 ± 5 W m^{-2} through acid addition to the regenerated catholyte to decrease pH and dissolve $Cu(OH)_2$ precipitates, suggesting that an inexpensive acid or a waste acid could be used to improve performance. These results demonstrated that TRABs using ammonia-based electrolytes and inexpensive copper electrodes can provide a practical method for efficient conversion of low-grade thermal energy into electricity.

Broader context

The utilization of waste heat for power production would enable additional electricity generation without any additional consumption of fossil fuels. Thermally regenerative batteries (TRBs) allow a carbon neutral approach for the storage and conversion of waste heat into electrical power, with potentially lower cost than solid-state devices. Here we present a highly efficient, inexpensive, and scalable ammonia-based TRB (TRAB) where electrical current is produced from the formation of copper ammonia complex. The ammonia can then be captured and concentrated by distillation of the electrolyte, allowing recharge of the system. The voltage created by ammonia addition in the anolyte results in copper deposition onto the cathode, and loss of copper from the anode. However, by reversing the function of electrodes in the next cycle, there is no net loss of copper. With a 3 M anolyte ammonia, a TRAB produced the highest power density ever obtained for an aqueous-based, thermoelectrochemical system, of 136±3 W m^{-2}. This power density was substantially higher than those produced using salinity gradient energy technologies based on generating salty and less-salty solutions using waste heat. This TRAB technology therefore represents a new and promising approach for efficient harvesting of low-grade waste heat as electrical power.

Introduction

Low-grade heat utilization has drawn increasing attention due to its potential for carbon-neutral electricity production. Large amounts of low-grade thermal energy (temperatures <130 °C) is available at many industrial sites, but this energy can also be produced from geothermal and solar-based processes.[1] Solid-state devices based on semiconductor materials have been extensively studied for direct thermal-electric energy conversion,[2] but they are expensive and lack the capacity for energy storage. Liquid-based thermoelectrochemical systems (TESs),[3] and systems based on salinity gradient energy (SGE),[4] offer potentially less expensive and scalable routes for direct thermal-electric energy conversion that also have the capacity for desirable energy storage. However, these TES and SGE processes have produced low power densities and energy efficiencies.[3, 4]

Power production in some TESs is accomplished from the cell voltage produced by a temperature gradient across two electrodes.[5-7] In addition to low power densities, relatively toxic or expensive materials have been used. A maximum power density of 1.45 W m^{-2} was produced in a TES using potassium ferrocyanide/ferricyanide redox solutions and carbon nanotube electrodes at a temperature difference of 60 °C (thermal energy efficiency of 0.25%, or 1.4% of the Carnot efficiency).[6] The use of ionic liquids enabled operation at higher temperatures (130 °C), but the maximum power densities reached only 0.5 W m^{-2} with a cobalt (II/III) tris(bipyridyl) ionic liquid and Pt black-coated electrodes.[5] TESs based on other approaches are being developed to improve the power production and energy efficiencies. In one approach, the TES electrodes were charged at a higher temperature, and discharged at a lower temperature. A relatively high thermal efficiency of 5.7% was obtained by cycling solutions between 10 and 60 °C, but we estimate the power density was still only ~5.6 W m^{-2} of Cu foil projected electrode area, when operated

between 10 – 80 °C.[8] Another type of TES recently developed, called a thermally regenerative battery (TRB), operated at a fixed temperature and used waste or low-grade heat sources to regenerate the electrolyte. A copper-based TRB was examined based on Cu comproportionation [Cu^{2+} + Cu + 8 ACN → 2 $Cu(ACN)_4^+$], using acetonitrile (ACN) to complex and stabilize Cu(I).[9] However, the high internal resistance of the system (30 Ω), due to low ion solubility in acetonitrile, limited the power density to a maximum of ~18 W m^{-2} (our estimate based on an open circuit voltage of 0.61 V). In addition, the cathode was platinum, and the copper anode corrosion was not reversible as regenerated Cu(0) could not be electrodeposited onto the electrode. The heat demand was large as both the anode and cathode electrolytes, separated by an ion exchange membrane, needed to be distilled to remove acetonitrile to allow Cu(I) to undergo disproportionation.

SGE technologies offer a different approach for capturing thermal energy as electrical power, which is based on difference in salinity between two solutions. Either natural salinity gradients can be used, or they can be artificially created by distillation of thermolytic solutions such as ammonium bicarbonate at relatively low temperatures (<60 °C).[10-13] The main SGE-based technologies being developed are reverse electrodialysis (RED), pressure retarded osmosis (PRO), and capacitive mixing (CapMix).[4, 14-17] Maximum power densities using SGE processes are generally in the range of 0.1 to 1 W m^{-2} (normalized to total membrane area) using RED,[16, 18] and 1 – 3.5 W m^{-2} using PRO with NaCl solutions at concentrations similar to those of seawater (0.6 M) and river water (12 mM).[19] An unusually high power density of 60 W m^{-2} was recently achieved with PRO, but only by using a very high NaCl concentration (3 M).[20] The main disadvantage of PRO and RED is that they use expensive membranes, and very large membrane areas are needed for power production. CapMix processes do not require membranes, but they

produce much less power than PRO or RED even when ion exchange polymers are used on the electrodes to capture energy based on Donnan potentials.[14, 15]

A different approach was developed here to generate electrical power from waste heat sources by combining different aspects of the TES and SGE approaches, called thermally regenerative ammonia-based battery (TRAB). In a TRAB, power generation was derived from the formation of metal ammine complexes, and produced by an ammonia concentration gradient that generated the potential difference, using inexpensive materials in completely regenerable cycles. In the TRAB, both electrodes made of solid copper [Cu (s)] are immersed in Cu(II) nitrate solutions, and they are alternately operated as anodes or cathodes in successive cycles. Ammonia (rather than ammonium carbonate in SGE processes) is added to the anolyte to produce a potential difference between the two copper electrodes (Figure 1), based on creating an ammine complex with Cu^{2+}, according to the electrode reactions:[21]

Cathode: Cu^{2+} (aq) + $2e^-$ → Cu (s) $E^0 = +0.340$ V

Anode: Cu (s) + 4 NH_3 (aq) → $Cu(NH_3)_4^{2+}$ (aq) + $2e^-$ $E^0 = -0.04$ V

Once the electrical power is discharged due to the complete overall reaction of Cu^{2+} (aq) + 4 NH_3 (aq) → $Cu(NH_3)_4^{2+}$ (aq), only the anolyte (as opposed to both electrolytes in the TRB) is treated in the distillation column to separate ammonia out from the effluent using waste heat to regenerate the electrolyte.[13] For example, at a typical vacuum distillation condition of 50 °C and 0.1 atm,[13] 97% of ammonia in a copper ammonia solution exists in the vapor phase (our estimate based on thermodynamic calculations using OLI studio software, for 0.1 M Cu^{2+} and 2 M NH_3). This concentrated ammonia stream is then re-dissolved in the spent catholyte to recharge the cell, and

re-deposit Cu (s) onto the electrode during the next discharge cycle. Thus, the spent catholyte chamber now becomes the anode chamber, achieving a closed-loop cycle with no net loss of Cu (s) from the electrodes (Figure 1). This cyclical process enables thermal energy in waste heat to be stored in an ammonia liquid stream, which can be added back into the electrolyte to recharge the battery and convert the thermal energy into the chemical energy stored in the battery. When needed, the battery can be discharged so that the stored chemical energy is effectively converted to electrical power. In this study, we primarily focused on the discharge aspects of the TRAB, and it is shown here that the TRAB approach has improved stability and performance than other TESs, and higher power densities than existing TES and SGE approaches.[9]

Results and discussion

Power production as a function of concentrations of ammonia and Cu(II). The performance of the TRAB was examined over a range of NH_3 and Cu(II) concentrations in a 5 M NH_4NO_3 supporting electrolyte. Increasing the anodic NH_3 concentration from 1 M to 3 M improved the power production from 57 ± 2 W m^{-2} to 136 ± 3 W m^{-2} (Figure 2A), mainly due the enhancement of anode performance (Figure 2B). Improved anode performance was consistent with the Nernst equation (Eq S1) as the anode potentials were more negative at increased NH_3 concentrations. Increasing NH_3 concentration from 1 to 3 M slightly reduced cathode overpotentials, although the reason for this decrease was not clear.

Changing Cu(II) concentrations of the electrolytes affected both anode and cathode potentials. A Cu(II) concentration of 0.1 M produced the highest power density of 115 ± 1 W m^{-2}, with a 2 M NH_3 anolyte (Figure 2). Reducing the Cu(II) concentration to 0.05 M slightly decreased power production to 110 ± 2 W m^{-2}, as the more negative cathode potentials was offset by the more

negative anode potentials. According to the Nernst equation (Eq S2), increasing the Cu(II) concentration should lead to more positive cathode and anode potentials, resulting in little change in performance. However, when the Cu(II) concentration was increased to 0.2 M, power decreased to 95 ± 6 W m^{-2}. This decrease was mainly due to the deterioration of the anode performance, as the cathode potentials were not appreciably affected (Figure 2).

Power production with different concentrations of the supporting electrolyte. The effect of the supporting electrolyte concentration was examined with 0.1 M Cu(II) and 1 M anolyte ammonia, by varying the NH_4NO_3 concentrations. Increasing the concentration of NH_4NO_3 generally increased the power production, with maximum power densities of 47 ± 2 W m^{-2} (3 M), 57 ± 2 W m^{-2} (5 M) and 55 ± 5 W m^{-2} (8 M) (Figure 3A). However, power production in the 8 M tests was more erratic, as seen by the higher standard deviations, than results at other concentrations. In addition, the power production at 8 M was similar to that obtained at 5 M. Increasing the concentration from 3 M to 8 M did not appreciably affect electrode potentials (Figure 3B), indicating that the reduction in solution resistance was the main reason for improved power production when increasing the NH_4NO_3 concentrations from 3 to 8 M. However, anode performance was greatly improved compared to operation of the TRAB without NH_4NO_3 addition (Figure S1). The use of concentrated NH_4^+ inhibited ammonia dissociation and improved ammonia activities, leading to more negative anode potentials. Both anode and cathode overpotentials greatly decreased with addition of NH_4NO_3 as the supporting electrolyte, due to the increase in solution conductivities (Figure S1). As reference electrodes were inserted outside the main current path, the measurement of electrode potentials included negligible ohmic potential drop, providing true electrode potentials.[22]

Stirring of the catholyte was needed to achieve high power densities during the discharge stage with 3–8 M NH_4NO_3 solutions (Figure 3). Otherwise, power overshoot was observed in the power curves (where the power curve bends back to lower current densities in the high current region; see Figure S1, for tests at 3, 5 and 8 M NH_4NO_3). Power overshoot occurred as a result of sharp decrease in the cathode potentials at high current densities, likely as a result of cathode concentration polarization. This phenomenon did not occur in the absence of NH_4NO_3, or at a lower concentration of 1 M NH_4NO_3, due to the lower current densities produced for these test conditions (Figure S1).

Electrochemical impedance spectroscopy (EIS) was used under a whole cell condition of 0.2 V to identify the components of cell impedance at different NH_4NO_3 concentrations. With increasing NH_4NO_3 concentrations, cell ohmic resistance decreased from 2.1 ± 0.1 Ω (3 M) to 1.4 ± 0.1 Ω (8 M), as a result of increased solution conductivity (Figure 4). However, this decrease in ohmic resistance was offset by an increase in the reaction resistance from 2.4 ± 0.1 Ω (3 M) to 3.5 ± 0.3 Ω (8 M) (Figure 4). This increase in reaction resistance that offset the benefit of reduced ohmic resistance was consistent with power production results showing that maximum power densities were not further improved when increasing the NH_4NO_3 concentration from 5 M to 8 M.

Cell scalability. To prove that multiple cells could be used to increase overall voltage and power production, two cells were connected in series and examined in polarization tests. With two cells, the maximum power production reached 36.0 ± 1.2 mW, which was double that obtained by a single cell (18.4 ± 0.1 mW; 5 M NH_4NO_3, 0.1 M $Cu(NO_3)_2$ electrolytes, and 2 M NH_3 in the anolyte) (Figure 5A). The electrode performance with the two-cell configuration was similar to that obtained by an individual cell (Figure 5B), showing that it was possible to connect multiple reactors in series to boost voltage and power production.

Cycling performance and energy efficiencies. Efficient transformation of waste heat into electrical power depends on consistent cell performance over multiple cycles. Therefore, power production by the TRAB was examined following electrolyte regeneration over three successive cycles [0.1 M Cu(II), 5 M NH_4NO_3 in both electrolytes and 2 M NH_3 in the anolyte]. Cells were operated at the load that produced the maximum power under these conditions (2.6 Ω external resistance), with the cycle terminated when the voltage was <20 mV. In the first cycle, with fresh electrolytes, the end of the cycle was due primarily to a sharp decrease in the cathode potential as a result of Cu^{2+} depletion (91±3% reduction) in the catholyte (Figure S2). The cathode coulombic efficiency was 102 ± 5% based on the mass change of the copper cathode, suggesting that Cu^{2+} reduction to Cu was the predominant reaction at the cathode. The anode coulombic efficiency was only 37 ± 4%, indicating that excess copper leached into the solution, likely due to dissolved oxygen being present as an alternate electron acceptor. The energy density in this initial cycle was 453 ± 28 Wh m^{-3} (normalized to the total electrolyte volume, or 61 ± 4 J cm^{-2} normalized to the projected surface area of a single electrode). The discharge energy efficiency was 44 ± 3 % (electrical energy captured versus chemical energy stored in the battery), but this efficiency is a function of the external resistance (electrical load), and therefore it likely could be increased with a larger external resistance.

For the second and successive cycles, ammonia was removed by heating the anolyte effluent (simulating distillation), and concentrated ammonia was added into the new anolyte. Stripping ammonia out of the anolyte effluent decreased the solution pH from ~9 to ~4.6. This resulted in formation of a precipitate in the electrolyte during this process due to the side reaction $Cu(NH_3)_4^{2+} + 4\ H_2O \rightarrow Cu(OH)_2\ (s) + 2\ NH_3{\cdot}H_2O + 2\ NH_4^+$. In the three successive regeneration cycles, this precipitate resulted in a similar but reduced peak power densities averaging 60 ± 3 W m^{-2} (61.7 ±

2.5 W m^{-2}, cycle 2; 55.9 ± 0.7 W m^{-2} , cycle 3; and 61.4 ± 0.8 W m^{-2}, cycle 4) (Figure 6). The lower power densities with the regenerated electrolyte were due to more negative reduction potentials of $Cu(OH)_2$/Cu (Figure S2B), as the cathode potential reflected the mixed potential of two reduction reactions: $Cu(OH)_2 + 2\ e^- \rightarrow Cu\ (s) + 2\ OH^-$ and $Cu^{2+} + 2\ e^- \rightarrow Cu\ (s)$. Similarly with the fresh electrolyte in the first cycle, the end of the cycle resulted from the decrease in the cathode potential due to the depletion of Cu(II) [i.e. Cu^{2+} and $Cu(OH)_2$] in the catholyte (Figure S2). The discharge energy efficiencies (captured electrical energy versus the stored chemical energy) remained high, averaging 29 ± 2 % (31 ± 2 %, cycle 2; 27 ± 0.4 %, cycle 3; and 29 ± 1 %, cycle 4) (Figure 6). Peak power densities and energy recoveries were relatively stable during the three regeneration cycles, showing good reproducibility with successive cycles. Longer-term performance over many more cycles will need to be established in a future study, but the data provided here establishes that in the short term, cycles can be reproducible. Acid was added into the regenerated catholyte to decrease the pH and dissolve the $Cu(OH)_2$. This increased the cell performance to 126 ± 5 W m^{-2}, and the discharge energy efficiency to 49 ± 2% (Figure 6). This effect of pH indicates that availability of a waste acid stream, or an inexpensive source of acid, might be used to achieve and maintain a higher cell performance than that possible using only a distillation process to regenerate the ammonia.

The total charge transferred in the second cycle (1100 ± 26 C) was double that of the first cycle (529 ± 16 C), due to the accumulated Cu(II) from the first cycle. An AEM was used to minimize mixing of Cu(II) species between the electrode chambers, thus the regenerated catholyte was more concentrated in Cu(II) due to copper corrosion in the previous cycle, and the regenerated anolyte had relatively depleted Cu(II). The charge increased with successive cycles, eventually exceeding the theoretical maximum (1156 C) based on the initial copper amount in the solution from the third

cycle (Figure 6). This increase in charge over successive cycles was consistent with the low anodic coulombic efficiencies, indicating that excess metal copper non-electrochemically oxidized and dissolved into the solution. As a result of increased charge, the energy density increased to 1054 ± 33 Wh m^{-3} at the fourth cycle. This excess copper corrosion by oxygen might also have affected the regeneration of the solution, as this reaction [$Cu\ (s) + 1/2\ O_2 + 4\ NH_3{\cdot}H_2O \rightarrow Cu(NH_3)_4^{2+} + 2\ OH^- + 3\ H_2O$] increased the solution pH, resulting in formation of $Cu(OH)_2$ during electrolyte regeneration. This precipitation problem could be mitigated by removal of dissolved oxygen from the solution, and by reducing oxygen leakage into the cell. The excess Cu(II) leaching into the solution could be recovered by other electrochemical technologies, such as cathodic reduction in microbial fuel cells,[23] or electrodeposition.[24]

The thermal energy needed for ammonia separation from the anolyte (2 M) was estimated to be 245 kWh/m^3-anolyte using the chemical process simulation software HYSYS. With a discharge energy density of 1054 ± 33 Wh m^{-3}, the thermal energy efficiency was 0.86%. This efficiency was much higher than that of 0.25% with the ferrocyanide/ferricyanide thermogalvanic cell,[6] and it could be further greatly enhanced by optimizing the TRAB operating temperature and active species concentrations in the future studies.

Experimental

Design, construction, and operation

A single TRAB cell consisted of anode and cathode chambers separated by an anion exchange membrane (AEM; Selemion AMV, Asashi glass, Japan; effective surface area of 7 cm^2) (Figure 1). The two chambers, each 4 cm long and 3 cm in diameter, were constructed from 4-cm cubes of Lexan.[25] The electrodes were made of copper mesh (50 × 50 mesh, McMaster-Carr, OH; 0.8

cm × 2 cm with a projected surface area of 1.6 cm^2, weight of 0.2365 ± 0.0004 g) connected using copper wires to an external resistor. Ag/AgCl reference electrodes (+211 mV versus SHE; RE-5B; BASi) were inserted at the two sides of the copper electrodes that were outside the current path to monitor the electrode potentials (Figure 1). The cathode chamber was stirred using a stir bar (6.4 × 15.9 mm, magnetic egg-shaped stir bars, VWR; 500 rpm) (except as noted otherwise) while the anolyte was not mixed.

The electrolyte was 0.1 M $Cu(NO_3)_2$ and 5 M NH_4NO_3 (Sigma Aldrich), except as noted, that were dissolved in deionized water. To charge the TRAB, 2 M ammonium hydroxide (Sigma-Aldrich, 5 N solution) was added to the anolyte to form the copper ammonia complex ion, although ammonia gas could also be used. In some experiments, the concentration of Cu(II) was varied from 0.05 M to 2 M, and the ammonia concentration varied from 1 M to 3 M, all in 5 M NH_4NO_3, to examine the effect of reactant concentrations on power production. In some experiments, NH_4NO_3 concentration was varied from 3 to 8 M to examine the effect of supporting electrolyte concentration on power production. The electrolyte conductivity increased from 256 mS/cm (3 M NH_4NO_3) to 397 mS/cm (8 M NH_4NO_3). The final pH of anolyte solutions decreased from 9.1 (3 M) to 8.7 (8 M), while the catholyte pH decreasing from 2.8 (3 M) to 2.4 (8 M) with the increasing NH_4NO_3 concentration (Figure S3).

In order to determine TRAB performance over multiple cycles, the cells were operated with a fixed 2.6 Ω external resistance for a whole batch cycle, which ended when the voltage was <20 mV. The effluent from two chambers was separately collected. The anolyte effluent was heated at 50 °C to distill the ammonia out to regenerate the catholyte for the next batch. Ammonia (in the form of ammonium hydroxide solution) was added to the catholyte effluent to form the new anolyte. All experiments were run in duplicate at room temperature (20 – 30 °C).

Calculations and measurements

Voltage across the external resistor (U), and electrode potentials versus the respective Ag/AgCl reference electrode (E_{cat}, E_{an}) were recorded at 1 min intervals using a data acquisition system (Agilent, Santa Clara, CA) connected to a personal computer. Polarization tests were performed by switching the external resistance every 5 min from 100.6 (or 40.6) to 1.6 Ω in decreasing order. Both current density ($I = U/RA$) and power density ($P = U^2/RA$) were normalized to a single electrode projected surface area (1.6 cm^2). Error bars indicate standard deviations for measurements using the duplicate reactors.

During the regeneration cycle tests, the total charge was calculated by integrating the current-time profile ($Q = \int It$), and total energy was calculated by integrating the power-time profile ($W = \int UIt$). Energy density was calculated by normalizing the total produced energy in one cycle by the total electrolyte volume (60 mL). Coulombic efficiency of the electrode was calculated as the ratio between actual produced charge and theoretical amount of charge based on the mass change of the electrode. For each piece of the electrode, the mass was measured 3 times using an analytical balance, and average values were used for the calculation.

The thermal-electrical energy conversion can be viewed as a two-step process with the TRAB. In the TRAB process, waste heat is first converted to the chemical energy stored in the battery during the charge process, which is then converted to electrical power during the discharge process. Therefore, we consider the efficiencies separately for the charge and discharge processes, similar to that of a rechargeable battery.[26] The energy efficiency for charge describes the energy conversion efficiency from thermal energy to chemical energy stored in the battery, while the energy efficiency for discharge is the ratio between discharged electrical energy and the chemical

energy stored in the battery. For the charge processes, the thermal energy needed for ammonia separation from the anolyte effluent was estimated based on the energy needed for separation of copper ammine complex and distillation energy of ammonia from the anolyte. Distillation of the electrolyte was modeled simply as a binary mixture of ammonia and water using Aspen HYSYS (Cambridge, MA) with a single distillation column, with the reboiler temperature set at 70.6 °C, and a column pressure drop of 0.15 atm. The column energy duty was reported by normalizing to the anolyte liquid volume, rather than the total electrolyte volume. We neglected the part of energy due to copper ammine complex separation, as it was much smaller than the column energy duty. The chemical energy stored in the solution was determined based on the ΔG of the overall cell reaction: $Cu^{2+} + 4\ NH_3\ (aq) \rightarrow Cu(NH_3)_4^{2+}\ (aq)$. The activities of the chemical species were estimated using the Visual MINTEQ software. At 25 °C, with 0.1 M Cu(II) in both electrolytes and 2 M anolyte ammonia, the ΔG was –74.9 kJ mol^{-1}, for a theoretical energy density in the starting solutions of 1040 Wh m^{-3} (normalized to the total electrolyte volume of 60 mL). As Cu(II) concentrations increased in the regenerated electrolyte, the theoretical energy density was calculated based on the Cu(II) concentration in the regenerated electrolyte that was estimated based on charge production assuming all catholyte Cu(II) was reduced in that cycle. The discharge energy efficiency was then calculated as the ratio between actual energy density produced in one cycle and the theoretical energy density ($\eta_{discharge}$ = actual energy density/ theoretical energy density). The thermal energy efficiency was calculated as the ratio between the discharge energy and the required thermal energy for electrolyte regeneration estimated in the HYSYS software ($\eta_{thermal}$ = actual discharge energy/ required thermal energy).

Electrochemical impedance spectroscopy (EIS) was performed with whole cells set at 0.2 V, to compare the cell ohmic resistance and overall reaction resistance with different concentrations

of NH_4NO_3. All EIS tests were performed over a frequency range of 100 kHz to 10 mHz with a sinusoidal perturbation of 10 mV amplitude. Cells were discharged at 0.2 V for 10 min with stable current production before the addition of sinusoidal perturbation in EIS tests to assure a pseudo steady state. The EIS spectra were fitted into the equivalent circuit as described in Figure S4, to identify the solution/membrane resistance (R_s), charge transfer and diffusion resistance of the two electrodes. We defined the reaction resistance (R_{rxn}) as the sum of the charge transfer and diffusion resistances.[22]

Conclusions

This TRAB based on copper ammonia complex formation demonstrated successful conversion of low-grade thermal energy into electric power, with electrolytes that can be thermally regenerated and electrodes maintained using closed-loop cycles. The maximum power density of ~60 W m^{-2} achieved here over successive cycles is substantially higher than that previously obtained in liquid-based thermal-electric energy conversion systems (< 10 W m^{-2}),[5-8] and higher than those typically produced using SGE technologies.[4, 14-17] An inexpensive source of acid would be needed to further increase power densities to 126 ± 5 W m^{-2} using the current process. The energy density of 453 ± 28 Wh m^{-3}, requiring only ammonia and a single membrane between the electrodes, was much higher than that previously obtained with a 20-cell pair RED using ammonia bicarbonate solutions (118 Wh m^{-3}).[16] The energy density over 1 kWh m^{-3} in the regenerated cycles suggested that energy density could be greatly improved by increasing the Cu(II) concentration in the electrolyte. The setup and operation of the TRAB are relatively simple, the reactants and electrode material are widely available and relatively inexpensive, and they do not require complex preparation processes or the use of expensive materials such as multiwall carbon nanotubes [6] or platinum.[9]

This TRAB system is not yet optimized, and therefore modifications could lead to reduced material costs or improved performance. For example, the AEM used to prevent the mixing of Cu(II) species between anolyte and catholyte solutions could be replaced by a less expensive battery-type separator. The TRAB could also be run in continuous flow mode as done for RED and flow electrode systems, the distillation and operating temperatures could be optimized, and the solution chemistry could be changed to further improve the cycling performance. Overall, this TRAB technology, based on an ammonia electrolyte and inexpensive metal electrodes, represents a new and promising approach for efficient conversion of low-grade waste heat to electrical power.

Acknowledgments

The authors thank David Jones for help with the analytical measurements. We also thank Nicole LaBarge for the HYSYS simulation, Dr. Marta Hatzell, Dr. Mike Hickner and Dr. Christopher Gorski for useful discussions. This research was supported by Award KUS-I1-003-13 from the King Abdullah University of Science and Technology (KAUST).

References

1. M. I. Hoffert, K. Caldeira, G. Benford, D. R. Criswell, C. Green, H. Herzog, A. K. Jain, H. S. Kheshgi, K. S. Lackner, J. S. Lewis, H. D. Lightfoot, W. Manheimer, J. C. Mankins, M. E. Mauel, L. J. Perkins, M. E. Schlesinger, T. Volk and T. M. L. Wigley, *Science*, 2002, **298**, 981-987.
2. L. E. Bell, *Science*, 2008, **321**, 1457-1461.
3. B. Anderson L, A. Greenberg S and B. Adams G, in *Regenerative EMF Cells*, American Chemical Society, 1967, vol. 64, ch. 15, pp. 213-276.

4. J. W. Post, J. Veerman, H. V. M. Hamelers, G. J. W. Euverink, S. J. Metz, K. Nymeijer and C. J. N. Buisman, *J. Membr. Sci.*, 2007, **288**, 218-230.
5. T. J. Abraham, D. R. MacFarlane and J. M. Pringle, *Energy Environ. Sci.*, 2013, **6**, 2639-2645.
6. R. Hu, B. A. Cola, N. Haram, J. N. Barisci, S. Lee, S. Stoughton, G. Wallace, C. Too, M. Thomas, A. Gestos, M. E. d. Cruz, J. P. Ferraris, A. A. Zakhidov and R. H. Baughman, *Nano Lett.*, 2010, **10**, 838-846.
7. T. J. Abraham, N. Tachikawa, D. R. MacFarlane and J. M. Pringle, *PCCP*, 2014, **16**, 2527-2532.
8. Seok Woo Lee, Yuan Yang, Hyun-Wook Lee, Hadi Ghasemi, Daniel Kraemer, Gang Chen and Y. Cui, *Nat. Commun.*, 2014, **5**.
9. P. Peljo, D. Lloyd, N. Doan, M. Majaneva and K. Kontturi, *PCCP*, 2014, **16**, 2831-2835.
10. M. Marino, L. Misuri, A. Carati and D. Brogioli, *Appl. Phys. Lett.*, 2014, **105**, -.
11. M. M. Marino, L.; Carati, A.; Brogioli, D., *eprint arXiv:1403.4049*, 2014.
12. A. Carati, M. Marino and D. Brogioli, *eprint arXiv:1309.3643*, 2013.
13. R. L. McGinnis, J. R. McCutcheon and M. Elimelech, *J. Membr. Sci.*, 2007, **305**, 13-19.
14. B. B. Sales, M. Saakes, J. W. Post, C. J. N. Buisman, P. M. Biesheuvel and H. V. M. Hamelers, *Environ. Sci. Technol.*, 2010, **44**, 5661-5665.
15. D. Brogioli, R. Ziano, R. A. Rica, D. Salerno, O. Kozynchenko, H. V. M. Hamelers and F. Mantegazza, *Energy Environ. Sci.*, 2012, **5**, 9870-9880.
16. M. C. Hatzell, I. Ivanov, R. D. Cusick, X. Zhu and B. E. Logan, *PCCP*, 2014, **16**, 1632-1638.
17. R. D. Cusick, Y. Kim and B. E. Logan, *Science*, 2012, **335**, 1474-1477.
18. J. W. Post, H. V. M. Hamelers and C. J. N. Buisman, *Environ. Sci. Technol.*, 2008, **42**, 5785-5790.

19. A. Achilli and A. E. Childress, *Desalination*, 2010, **261**, 205-211.
20. A. P. Straub, N. Y. Yip and M. Elimelech, *Environ. Sci. Technol. Lett.*, 2013, **1**, 55-59.
21. A. J. Bard, R. Parsons and J. Jordan, eds., *Standard potentials in aqueous solution*, Marcel Dekker, New York, 1985.
22. F. Zhang, J. Liu, I. Ivanov, M. C. Hatzell, W. Yang, Y. Ahn and B. E. Logan, *Biotechnol. Bioeng.*, 2014, in press.
23. A. T. Heijne, F. Liu, R. v. d. Weijden, J. Weijma, C. J. N. Buisman and H. V. M. Hamelers, *Environ. Sci. Technol.*, 2010, **44**, 4376-4381.
24. A. Mecucci and K. Scott, *J. Chem. Technol. Biotechnol.*, 2002, **77**, 449-457.
25. H. Liu and B. E. Logan, *Environ. Sci. Technol.*, 2004, **38**, 4040-4046.
26. J. Kang, F. Yan, P. Zhang and C. Du, *J. Power Sources*, 2012, **206**, 310-314.

Figure legends

Figure 1. Schematic of the TRAB to convert waste heat into electricity. Four steps form the closed-cycle system for harvesting waste heat: ① power production with the initial Cu(II) solution and the Cu(II) ammonia complex solution (formed by addition of ammonia into the copper solution); ② Regeneration of the electrolyte by waste heat; ③ power production with regenerated electrolyte, which also regenerates the electrode; ④ regeneration of the electrolyte by waste heat.

Figure 2. (A) Power production and (B) electrode potentials with various Cu(II) and ammonia concentrations, using 5 M NH_4NO_3 as the supporting electrolyte. Error bars represent standard deviations based on measurements with duplicate reactors.

Figure 3. (A) Power production and (B) electrode potentials with different concentrations of NH_4NO_3 as the supporting electrolyte, with 0.1 M Cu(II) in both electrolyte and 1 M ammonia in the anolyte. Error bars represent standard deviations based on measurements with duplicate reactors.

Figure 4. Nyquist plots of the whole cell impedance at 0.2 V with 3 – 8 M NH_4NO_3, all with 0.1 M Cu(II) and 1 M ammonia anolyte. The inserted figure represents the components of the impedance obtained by fitting the Nyquist spectra to the equivalent circuit described in Figure S4.

Figure 5. (A) Power production and (B) electrode potentials of two cells that were connected in series, in comparison with the single cell operation. Electrolyte contained 0.1 M Cu(II) with 2 M ammonia in the anolyte, and 5 M NH_4NO_3 as supporting electrolyte. Error bars represent standard deviations based on measurements with duplicate reactors.

Figure 6. Performance of the TRAB over successive cycles. Initial electrolyte contained 0.1 M Cu(II), 5 M NH_4NO_3 and additional 2 M NH_3 in the anolyte. The spent electrolyte was then regenerated and operated for 3 successive cycles. "With acid" stands for the condition where acid was added to the regenerated catholyte to fully dissolve $Cu(OH)_2$ that was formed during the regeneration. The dashed line indicates the theoretical limit of total charge based on the initial Cu(II) concentration. (See Figure S2 for complete cycle profiles.)

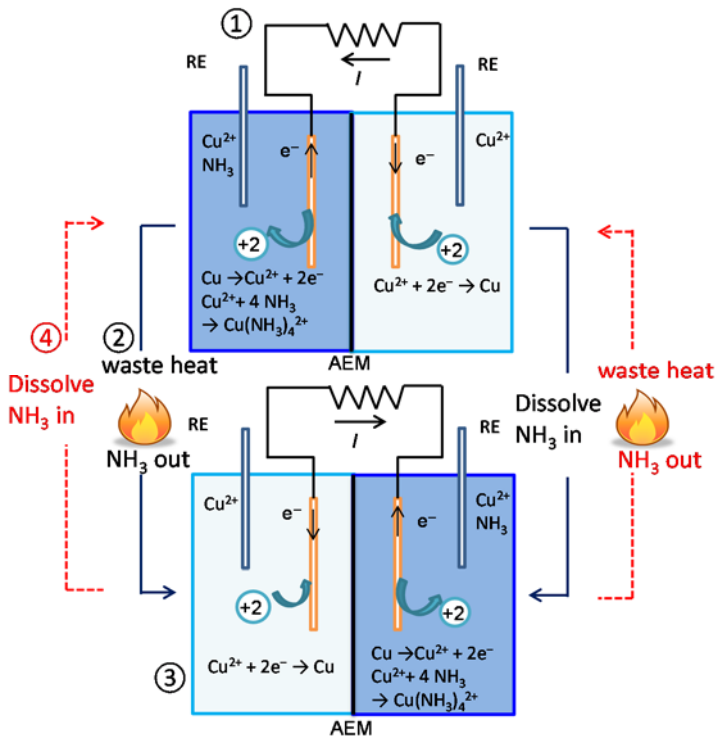

Figure 1. Schematic of the TRAB to convert waste heat into electricity. Four steps form the closed-cycle system for harvesting waste heat: ① power production with the initial Cu(II) solution and the Cu(II) ammonia complex solution (formed by addition of ammonia into the copper solution); ② Regeneration of the electrolyte by waste heat; ③ power production with regenerated electrolyte, which also regenerates the electrode; ④ regeneration of the electrolyte by waste heat.

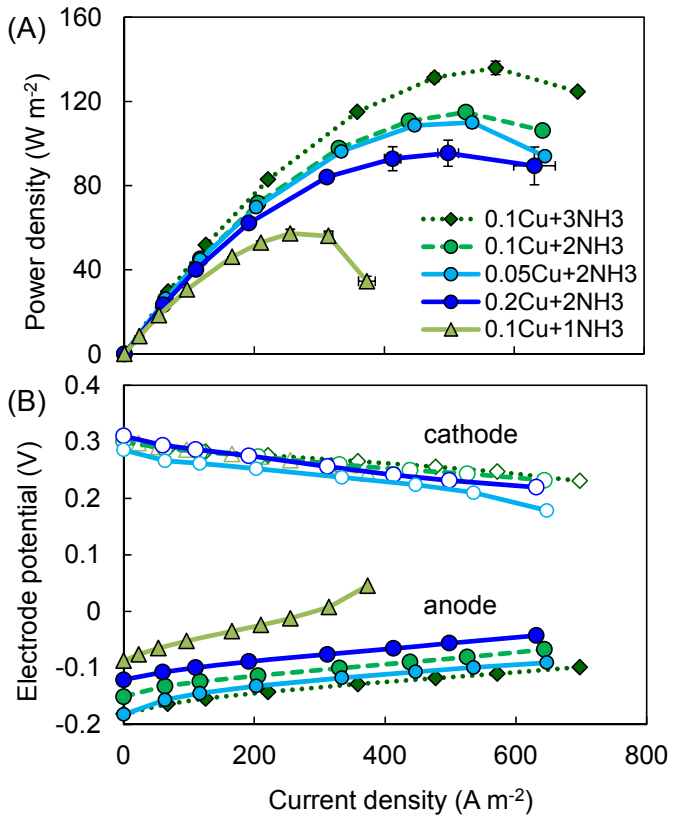

Figure 2. (A) Power production and (B) electrode potentials with various Cu(II) and ammonia concentrations, using 5 M NH_4NO_3 as the supporting electrolyte. Error bars represent standard deviations based on measurements with duplicate reactors.

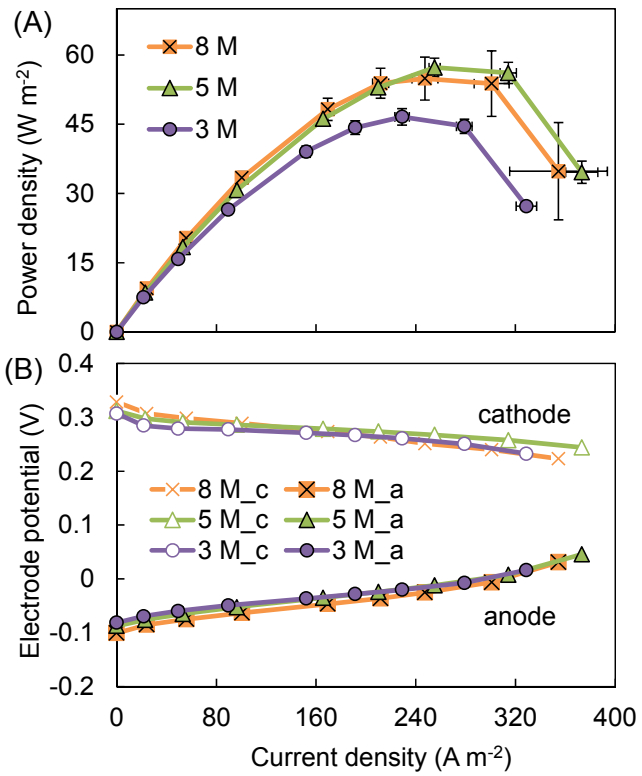

Figure 3. (A) Power production and (B) electrode potentials with different concentrations of NH_4NO_3 as the supporting electrolyte, with 0.1 M Cu(II) in both electrolyte and 1 M ammonia in the anolyte. Error bars represent standard deviations based on measurements with duplicate reactors.

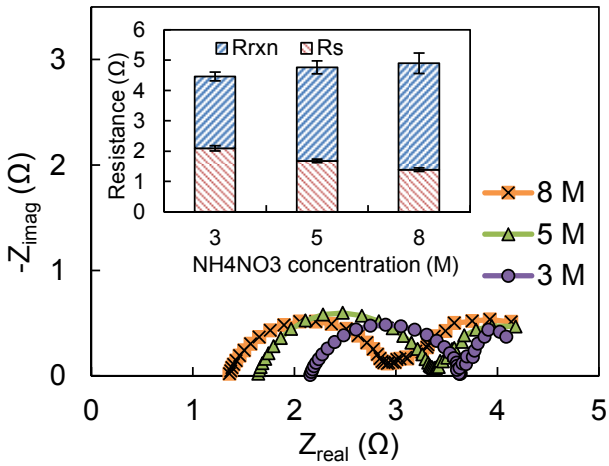

Figure 4. Nyquist plots of the whole cell impedance at 0.2 V with 3 – 8 M NH_4NO_3, all with 0.1 M Cu(II) and 1 M ammonia anolyte. The inserted figure represents the components of the impedance obtained by fitting the Nyquist spectra to the equivalent circuit described in Figure S4.

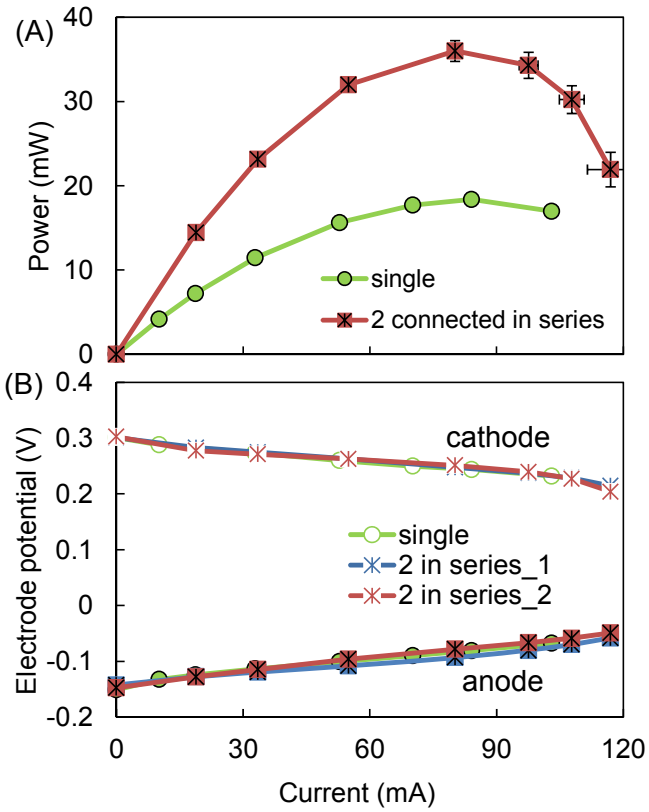

Figure 5. (A) Power production and (B) electrode potentials of two cells that were connected in series, in comparison with the single cell operation. Electrolyte contained 0.1 M Cu(II) with 2 M ammonia in the anolyte, and 5 M NH_4NO_3 as supporting electrolyte. Error bars represent standard deviations based on measurements with duplicate reactors.

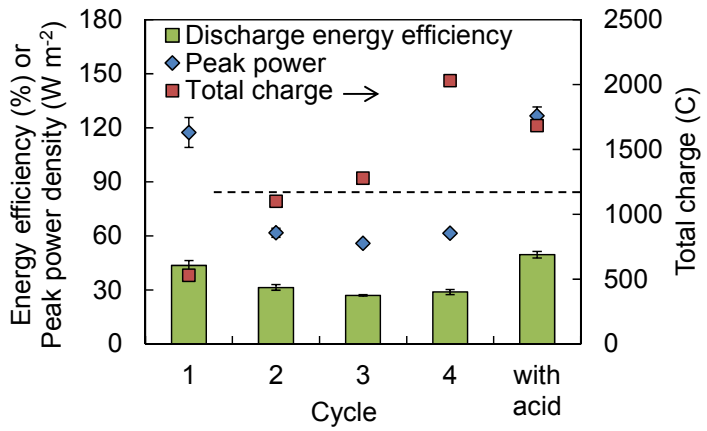

Figure 6. Performance of the TRAB over successive cycles. Initial electrolyte contained 0.1 M Cu(II), 5 M NH_4NO_3 and additional 2 M NH_3 in the anolyte. The spent electrolyte was then regenerated and operated for 3 successive cycles. "With acid" stands for the condition where acid was added to the regenerated catholyte to fully dissolve $Cu(OH)_2$ that was formed during the regeneration. The dashed line indicates the theoretical limit of total charge based on the initial Cu(II) concentration. (See Figure S2 for complete cycle profiles.)